

**NASA TECHNICAL  
MEMORANDUM**



**NASA TM X-3488**

**NASA TM X-3488**

**REEVALUATION OF COMPRESSIBLE-FLOW  
PRESTON TUBE CALIBRATIONS**

*Jerry M. Allen*

*Langley Research Center*

*Hampton, Va. 23665*

**U.S. AIR FORCE  
VAFB TECHNICAL LIBRARY**

1. Report No. NASA TM X-3488		2. Government Accession No.		3. Recipient's Catalog No.	
4. Title and Subtitle REEVALUATION OF COMPRESSIBLE-FLOW PRESTON TUBE CALIBRATIONS				5. Report Date February 1977	
				6. Performing Organization Code	
7. Author(s) Jerry M. Allen				8. Performing Organization Report No. L-11189	
				10. Work Unit No. 505-11-15-02	
9. Performing Organization Name and Address NASA Langley Research Center Hampton, VA 23665				11. Contract or Grant No.	
				13. Type of Report and Period Covered Technical Memorandum	
12. Sponsoring Agency Name and Address National Aeronautics and Space Administration Washington, DC 20546				14. Sponsoring Agency Code	
15. Supplementary Notes					
16. Abstract  Revised zero-pressure-gradient, adiabatic-wall skin-friction-balance data covering a Mach number range from 1.6 to 4.6 have led to a reevaluation of existing compressible-flow Preston tube calibration equations and a modification of the equations of Allen (NASA TN D-7190) and of Bradshaw and Unsworth (IC Aero. Rep. 73-07). It was found that the general results and conclusions obtained by Allen and by Bradshaw and Unsworth remain unchanged. However, some of the constants contained in the calibration equations developed in these two papers have been changed as a result of the revised skin-friction data.					
17. Key Words (Suggested by Author(s)) Preston tube calibrations Supersonic flow Boundary layer Skin-friction balance			18. Distribution Statement Unclassified - Unlimited  Subject Category 34		
19. Security Classif. (of this report) Unclassified		20. Security Classif. (of this page) Unclassified		21. No. of Pages 23	22. Price* \$3.25

# REEVALUATION OF COMPRESSIBLE-FLOW PRESTON TUBE CALIBRATIONS

Jerry M. Allen  
Langley Research Center

## SUMMARY

Revised zero-pressure-gradient, adiabatic-wall skin-friction-balance data covering a Mach number range from 1.6 to 4.6 have led to a reevaluation of existing compressible-flow Preston tube calibration equations and a modification of the equations of Allen (NASA TN D-7190) and of Bradshaw and Unsworth (IC Aero. Rep. 73-07). It was found that the general results and conclusions obtained by Allen and by Bradshaw and Unsworth remain unchanged. However, some of the constants contained in the calibration equations developed in these two papers have been changed as a result of the revised skin-friction data.

## INTRODUCTION

A few years ago the present author published the results of a study (refs. 1 and 2) in which existing supersonic, zero-pressure-gradient, adiabatic-wall, Preston tube calibration data from references 3 and 4 and new data generated by the author were used to evaluate existing calibration equations and to derive an improved equation. More recently, Bradshaw and Unsworth (refs. 5 and 6), in an attempt to derive a compressible-flow calibration equation which would give valid results in pressure-gradient flows, used the data from reference 1 to develop a calibration equation, based on inner law similarity, which is dependent only on flow conditions near the wall.

The data on which the results of these studies were based consisted of Preston tube and skin-friction-balance measurements obtained at similar flow conditions. The balance used to obtain the calibration data in reference 1 has been recently found to give friction values which are as much as 18 percent higher than those obtained with other, similar balances and also higher than theory values. These high friction values of course affected the evaluation of the existing calibration equations performed in reference 1 and also affected the two equations which were derived from these data - equation (36) of reference 1 and equation (6) of reference 5.

To investigate this anomaly a new set of skin-friction-balance data were obtained covering the test conditions of the reference 1 data, and comparisons were made with theory. These measurements confirmed that the balance used to obtain the reference 1 data did produce erroneously high skin-friction values and provided a new set of adiabatic-wall skin-friction calibration data.

The purpose of this paper is to use these new data to reevaluate the existing calibration equations and to modify the equations of Allen (ref. 1) and Bradshaw and Unsworth (ref. 5) to account for these more accurate balance data.

## SYMBOLS

a	speed of sound
$c_f$	local skin-friction coefficient, $\frac{\tau_w}{\frac{1}{2} \rho_e u_e^2}$
D	Preston tube outside diameter
$F_1$	calibration parameter, $\frac{\rho'}{\rho_e} \frac{\mu_e}{\mu'} R_D \frac{u_{pt}}{u_e}$
$F_2$	calibration parameter, $\sqrt{\frac{\rho'}{\rho_e}} \frac{\mu_e}{\mu'} R_D \sqrt{c_f}$
$F_3$	calibration parameter, $\frac{\rho_w}{\rho_e} \frac{\mu_e}{\mu_w} \frac{\sqrt{5 + M_e^2}}{M_e} R_D \sin^{-1} \left( \frac{M_e}{\sqrt{5 + M_e^2}} \frac{u_{pt}}{u_e} \right)$
$F_4$	calibration parameter, $\sqrt{\frac{\rho_w}{\rho_e}} \frac{\mu_e}{\mu_w} R_D \sqrt{c_f}$
$F_5$	calibration parameter, $\sqrt{\frac{\rho'}{\rho_e}} \frac{\mu_e}{\mu'} R_D \frac{M_{pt}}{M_e}$
M	Mach number, $\frac{u}{a}$
$M_\tau$	friction Mach number, $\frac{\sqrt{\tau_w}}{a_w \sqrt{\rho_w}}$
$P_\tau$	calibration parameter, $\frac{p_{pt} - p_w}{\tau_w}$
p	pressure
$R_D$	Reynolds number based on Preston tube diameter, $\frac{\rho_e u_e D}{\mu_e}$
$R_\theta$	Reynolds number based on momentum thickness, $\frac{\rho_e u_e \theta}{\mu_e}$
$R_\tau$	calibration parameter, $\frac{D}{\mu_w} \sqrt{\tau_w \rho_w}$
u	velocity in streamwise direction
$\theta$	boundary-layer momentum thickness
$\mu$	viscosity
$\rho$	density

$\tau$  shearing stress

Subscripts:

c calculated from calibration equation  
 e boundary-layer edge  
 m measured by skin-friction balance  
 pt measured by Preston tube  
 w wall

Primes denote fluid properties evaluated at reference temperature using the Sommer and Short method. (See ref. 7.)

NEW CALIBRATION DATA

The inaccuracies contained in the data of reference 1 are illustrated in figure 1. A Kistler skin-friction balance, serial number (SN) 222, was used to obtain those data, which are included in the SN 222 band of data shown in figure 1. This band was drawn from several different sets of data obtained with this balance and shows that the SN 222 balance has consistently produced results which are higher than theory.

Figure 1 also shows recent data from two other, similar balances (designated Kistler balances SN 223 and SN 225) covering the same flow conditions as the reference 1 data. These newer data agree much better with theory than the reference 1 data. Hence, it appears that the balance used to obtain the friction data used in reference 1 yielded erroneously high results. More accurate calibrations would be obtained by making use of the new data. Since the SN 223 and SN 225 data in figure 1 agree well with theory, the skin-friction values chosen to reduce the Preston tube data of reference 1 were taken from the Karman-Schoenherr curve at the measured transformed Reynolds numbers. The following table shows a comparison between these new skin-friction values taken from figure 1 and the original data used in reference 1:

$M_e$	$Re$	$C_f$ used in present paper (a)	$C_f$ from reference 1
1.975	$3.62 \times 10^4$	0.00156	0.00176
2.320	1.48	.00168	.00182
	2.38	.00154	.00176
	4.42	.00138	.00163
	6.41	.00130	.00154
	8.04	.00125	.00147
4.630	1.07	.00102	.00103
	1.69	.00094	.00099
	3.11	.00083	.00090
	4.44	.00078	.00088
	5.71	.00075	.00086
	6.81	.00073	.00084

<sup>a</sup>Obtained from Karman-Schoenherr theory.

The difference between the old and new skin-friction values is as much as 18 percent at the higher Reynolds numbers.

### EVALUATION OF EXISTING CALIBRATION EQUATIONS

The calibration equations evaluated in reference 1 will now be reexamined using the new skin-friction results presented in the previous table. As was done in reference 1, the data of Hopkins and Keener (ref. 3) and Fenter and Stalmach (ref. 4) also will be used in the evaluations. Also, as in reference 1, the Sommer and Short reference temperature (ref. 7) and the Sutherland viscosity law were employed in the data reduction. Since the largest differences between the old and new skin-friction values occurred at the higher Reynolds numbers, the primary concern of this reevaluation will be the performance of the various calibration equations at the higher values of the calibration parameters, that is, at the higher Reynolds numbers. Plots of the data and equations will be analyzed for two characteristics: (1) the capability of the calibrating parameters to collapse the data onto a single band and (2) the accuracy of the fit of the calibration equations to the experimental data. Agreement in skin friction between data and theory of about  $\pm 10$  percent is generally considered very good in Preston tube measurements.

#### Fenter-Stalmach Equation

The three independent sets of experimental data are plotted in figure 2(a) using the calibration parameters  $F_3$  and  $F_4$  used by Fenter and Stalmach (ref. 4) and are compared with the values obtained from the equation

$$F_3 = F_4(4.06 \log_{10} F_4 + 1.77) \quad (1)$$

where

$$F_3 = \frac{\rho_w}{\rho_e} \frac{\mu_e}{\mu_w} \frac{\sqrt{5 + M_e^2}}{M_e} R_D \sin^{-1} \left( \frac{M_e}{\sqrt{5 + M_e^2}} \frac{u_{pt}}{u_e} \right)$$

and

$$F_4 = \sqrt{\frac{\rho_w}{\rho_e}} \frac{\mu_e}{\mu_w} R_D \sqrt{C_f}$$

The data collapse is good, and the equation fits the data fairly well except at the higher Reynolds numbers (higher values of the calibration parameters).

It is difficult from figure 2(a) to ascertain the accuracy with which the equation predicts the measured skin friction. Figure 2(b) was thus prepared to more clearly show the agreement between data and theory. The general trend is for the calculated skin friction to be higher than the measured skin friction throughout the range of  $F_3$ . As was done in reference 1, data for  $F_3 < 10^3$  (or  $F_2 < 10^2$ ) are not considered in assessing the accuracy of the calibration equations in this paper. Hopkins and Keener in reference 3 noticed large deviations

in their data when  $F_2 < 10^2$  and recommended  $F_2 = 10^2$  as the lower limit for the Preston tube technique.

### Sigalla Equation

Figure 3(a) shows how the experimental data compare with the values obtained with the Sigalla calibration equation (from ref. 8)

$$F_1 = 5.13(F_2)^{1.146} \quad (2)$$

where

$$F_1 = \frac{\rho_t}{\rho_e} \frac{\mu_e}{\mu_t} R_D \frac{u_{pt}}{u_e}$$

and

$$F_2 = \sqrt{\frac{\rho_t}{\rho_e}} \frac{\mu_e}{\mu_t} R_D \sqrt{c_f}$$

The calibration parameters  $F_1$  and  $F_2$  used by Sigalla collapse the data onto a single band with about the same amount of scatter as was present in the calibration parameters  $F_3$  and  $F_4$  used by Fenter and Stalmach. The Sigalla equation fits the data fairly well except at the higher Reynolds numbers. In terms of percent skin-friction error, figure 3(b) shows that the equation misses the trend of the data at these higher Reynolds numbers.

### Hopkins-Keener Equation

Figure 4(a) shows how the experimental data compare with the values obtained with the Hopkins-Keener equation (from ref. 3)

$$F_5 = 5.74(F_2)^{1.132} \quad (3)$$

where

$$F_5 = \sqrt{\frac{\rho_t}{\rho_e}} \frac{\mu_e}{\mu_t} R_D \frac{M_{pt}}{M_e}$$

The calibration parameters  $F_2$  and  $F_5$  used by Hopkins and Keener do not collapse the data onto a single band at the higher Reynolds numbers. This effect was noted in reference 1 and is still present with these revised data.

This divergence between measured and calculated skin friction can be seen more clearly in figure 4(b). Of all the calibration parameters tested in this paper, only those used by Hopkins and Keener resulted in such a large deviation from a single band.



### Patel T' Equation

The calibration parameters  $F_1$  and  $F_2$  used in the Patel T' equation (derived in ref. 1)

$$F_1 = F_2(3.91 \log_{10} F_2 + 2.34) \quad (4)$$

are the same as those used by Sigalla and, therefore, the data collapse is equally good. Figure 5(a) shows that the Patel T' equation fits the data fairly well except at the higher Reynolds numbers. Figure 5(b) shows that the calculated skin-friction values are, overall, somewhat larger than the measured values.

### MODIFICATION TO EQUATIONS DERIVED FROM REFERENCE 1 DATA

#### Allen Equation

In order to obtain the best possible curve fit to the data, a least-squares curve-fitting technique was employed in reference 1. A similar procedure will be employed in this paper to fit the best possible curve to the revised data. As in reference 1, the calibration parameters  $F_1$  and  $F_2$  were chosen for the curve fit because of the good data collapse provided by these parameters. The calibration parameters  $F_3$  and  $F_4$  also gave good data collapse but were not chosen because they are restricted to adiabatic-wall conditions, as explained in reference 1. Choosing  $F_1$  and  $F_2$ , therefore, did not exclude the possibility that the resulting calibration equation could be used under heat transfer conditions. All three sets of data were used, but the curve fit includes only those data whose  $F_2$  values are greater than  $10^2$ .

A linear least-squares curve was tried to the log-log plot first, and the results are shown in figure 6(a). The equation of this fit is

$$F_1 = 5.85(F_2)^{1.132} \quad (5)$$

This curve misses the trend of the data somewhat at the higher Reynolds numbers, as can be seen more clearly in terms of skin-friction error from figure 6(b).

To represent the data more accurately a second-order least-squares curve fit was obtained and is shown in figure 7(a). The equation of this curve is

$$\log_{10} F_2 = 0.01239(\log_{10} F_1)^2 + 0.7814 \log_{10} F_1 - 0.4723 \quad (6)$$

The second-order term in this equation enables the curve to fit the data quite well even at the higher Reynolds numbers, as can be seen more easily in the skin-friction-error plot of figure 7(b).

A third-order least-squares curve fit was obtained, but no noticeable improvement in accuracy was seen. Hence equation (6) appears to be the best least-squares fit to the data using the  $F_1$  and  $F_2$  calibration parameters. Note that equation (6) is of the same form as equation (36) of reference 1, which was recommended in that paper as the best curve fit to the data that

existed at that time. The only differences between the two equations are slight adjustments to the constants caused by the revised data in this paper.

### Bradshaw-Unsworth Equation

In reference 5 Bradshaw and Unsworth, using the data from reference 1, developed a new calibration equation based entirely on conditions near the wall. This new equation had the advantage of being potentially valid for pressure-gradient flows. It had a disadvantage, however, in that its solution required an iteration procedure. Since the data in reference 1 has been adjusted in the present paper, the constants in the Bradshaw-Unsworth equation required modification to account for these revised data. The following equation was thus developed by using the same derivation procedure used by Bradshaw and Unsworth with the revised data of the present paper:

$$P_{\tau} = 96 + 60 \log_{10} \left( \frac{R_{\tau}}{50} \right) + 2.37 \left[ \log_{10} \left( \frac{R_{\tau}}{50} \right) \right]^2 + 10^4 M_{\tau}^2 (R_{\tau}^{0.30} - 2.38) \quad (7)$$

where

$$P_{\tau} = \frac{p_{pt} - p_w}{\tau_w}$$

$$M_{\tau} = \frac{\sqrt{\tau_w}}{a_w \sqrt{\rho_w}}$$

$$R_{\tau} = \frac{D}{\mu_w} \sqrt{\tau_w \rho_w}$$

The only difference between equation (7) and the original Bradshaw-Unsworth equation (eq. (6) of ref. 5) is in the last term. The expression  $(R_{\tau}^{0.30} - 2.38)$  in equation (7) has replaced  $(R_{\tau}^{0.26} - 2.00)$  in the original equation. Thus equation (7), like the original Bradshaw-Unsworth equation in reference 5, requires iteration to solve for  $c_f$ .

Since the Bradshaw-Unsworth equation contains three parameters ( $P_{\tau}$ ,  $R_{\tau}$ , and  $M_{\tau}$ ), it is not possible to show graphically the data collapse; however, the percent skin-friction error can be shown and is presented in figure 8 for all three sets of data. Since only the revised data of the present report were used in the derivation of equation (7), the curve fit to these data is somewhat better than to the other two sets of data.

The curve fit to all three sets of data, however, is fairly good and is only marginally inferior to the fit of the second-order least-squares curve (eq. (6)) developed in this paper, as can be seen by comparing figures 7(b) and 8. Note from these figures that both equations (6) and (7) give valid results even at the largest Preston tube diameters tested (largest  $F_1$  values), which were as large as 70 percent of the boundary-layer thickness.

## CONCLUSIONS

Revised skin-friction-balance data have led to a reevaluation of existing adiabatic-wall compressible-flow Preston tube calibrations and a modification of the equations of Allen and of Bradshaw and Unsworth. Based on the results of this study, the following conclusions have been drawn:

1. The general results and conclusions obtained by Allen (NASA TN D-7190) and by Bradshaw and Unsworth (IC Aero. Rep. 73-07) remain unchanged; however, some of the constants contained in the calibration equations developed in these two papers have been changed as a result of the revised skin-friction data contained in the present paper.

2. Of all the Preston tube calibration equations evaluated in this paper, the revised equations of Allen and of Bradshaw and Unsworth gave the most accurate results.

3. The Allen equation has the advantage of being able to solve explicitly for skin friction, whereas the Bradshaw-Unsworth equation requires iteration.

4. The Bradshaw-Unsworth equation has the advantage of being based entirely on conditions near the wall (no knowledge of free-stream conditions is required); therefore, it is potentially valid in pressure-gradient flows.

5. Both the Allen and the Bradshaw-Unsworth equations give valid results for Preston tubes as large as 70 percent of the boundary-layer thickness.

Langley Research Center  
National Aeronautics and Space Administration  
Hampton, VA 23665  
December 13, 1976

## REFERENCES

1. Allen, Jerry M.: Evaluation of Compressible-Flow Preston Tube Calibrations. NASA TN D-7190, 1973.
2. Allen, Jerry M.: Evaluation of Preston Tube Calibration Equations in Supersonic Flow. AIAA J., vol. 11, no. 11, Nov. 1973, pp. 1461-1462.
3. Hopkins, Edward J.; and Keener, Earl R.: Study of Surface Pitots for Measuring Turbulent Skin Friction at Supersonic Mach Numbers - Adiabatic Wall. NASA TN D-3478, 1966.
4. Fenter, Felix W.; and Stalmach, Charles J., Jr.: The Measurement of Local Turbulent Skin Friction at Supersonic Speeds by Means of Surface Impact Pressure Probes. DRL-392, CM-878 (Contract NOrd-16498), Univ. of Texas, Oct. 21, 1957.
5. Bradshaw, P.; and Unsworth, K.: A Note on Preston Tube Calibrations in Compressible Flow. IC Aero. Rep. 73-07, Dep. Aeronaut., Imperial College Sci. & Technol., Sept. 1973.
6. Bradshaw, P.; and Unsworth, K.: Comment on "Evaluation of Preston Tube Calibration Equations in Supersonic Flow." AIAA J., vol. 12, no. 9, Sept. 1974, pp. 1293-1295.
7. Sommer, Simon C.; and Short, Barbara J.: Free-Flight Measurements of Turbulent-Boundary-Layer Skin Friction in the Presence of Severe Aerodynamic Heating at Mach Numbers From 2.8 to 7.0. NACA TN 3391, 1955.
8. Sigalla, Armand: Calibration of Preston Tubes in Supersonic Flow. AIAA J., vol. 3, no. 8, Aug. 1965, p.1531.

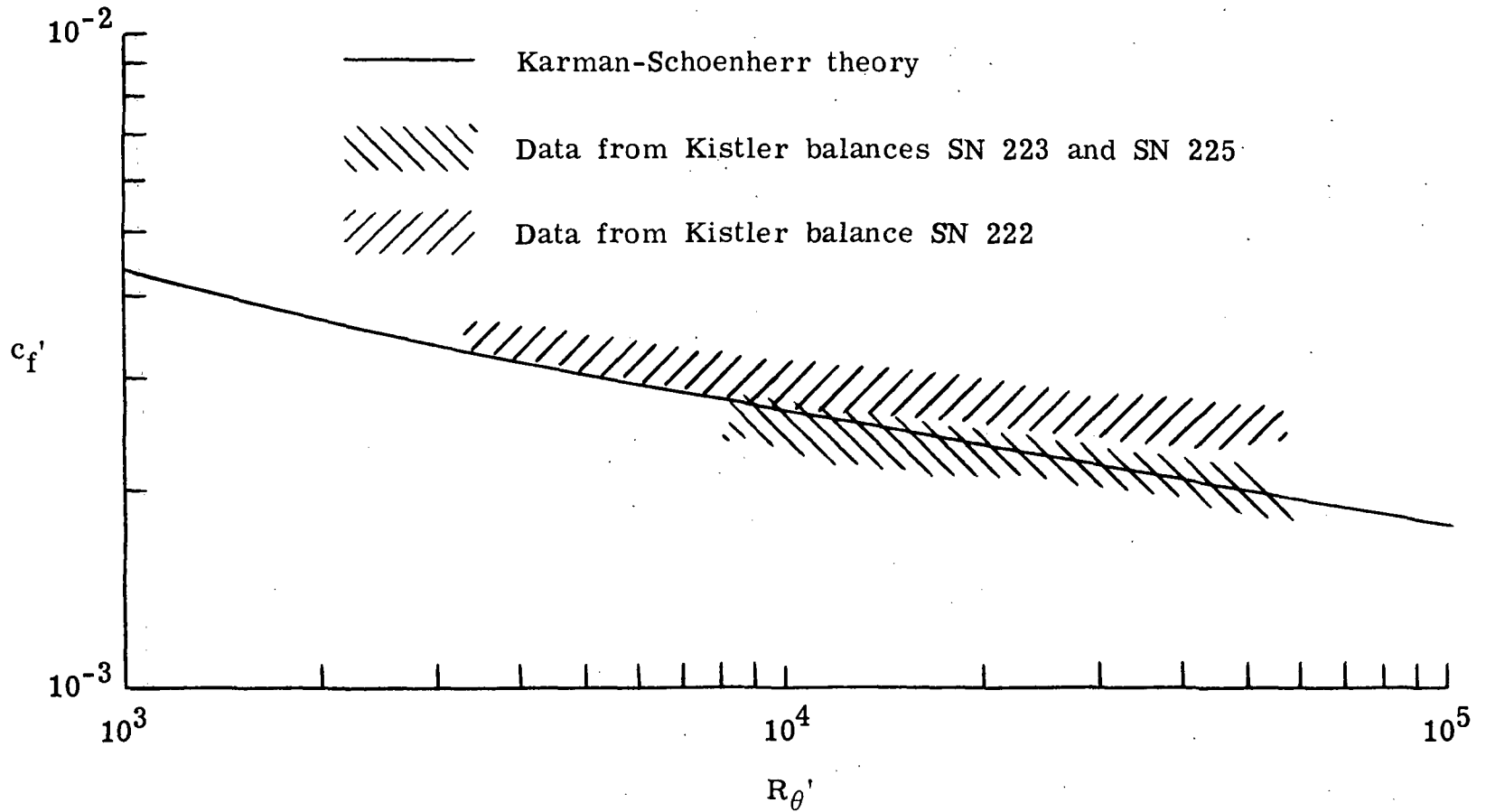
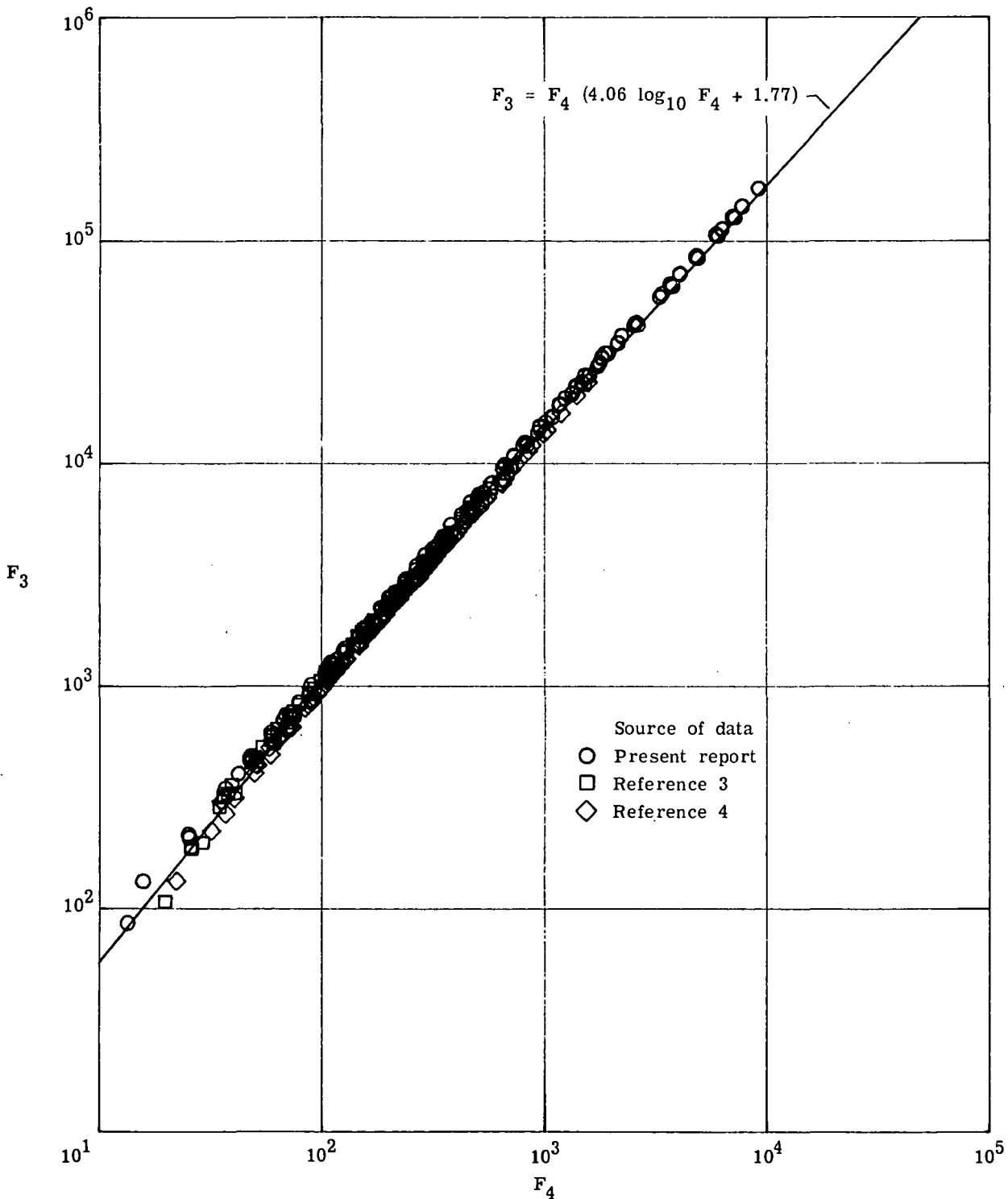
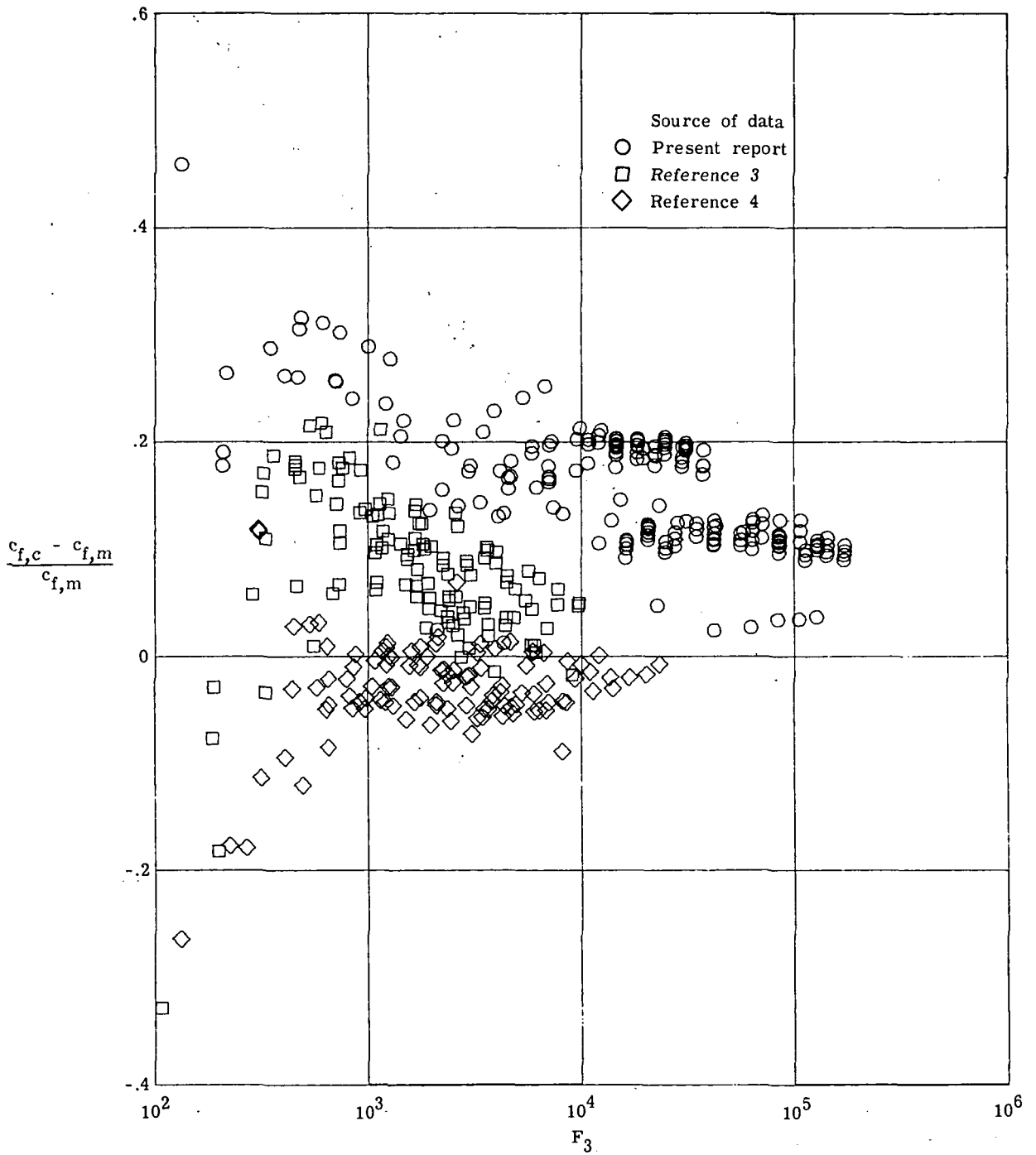


Figure 1.- Skin-friction data obtained using Kistler balances SN 222, SN 223, and SN 225.  
 $1.6 < M_e < 4.6$ ;  $10^4 < R_{\theta} < 8 \times 10^4$ .



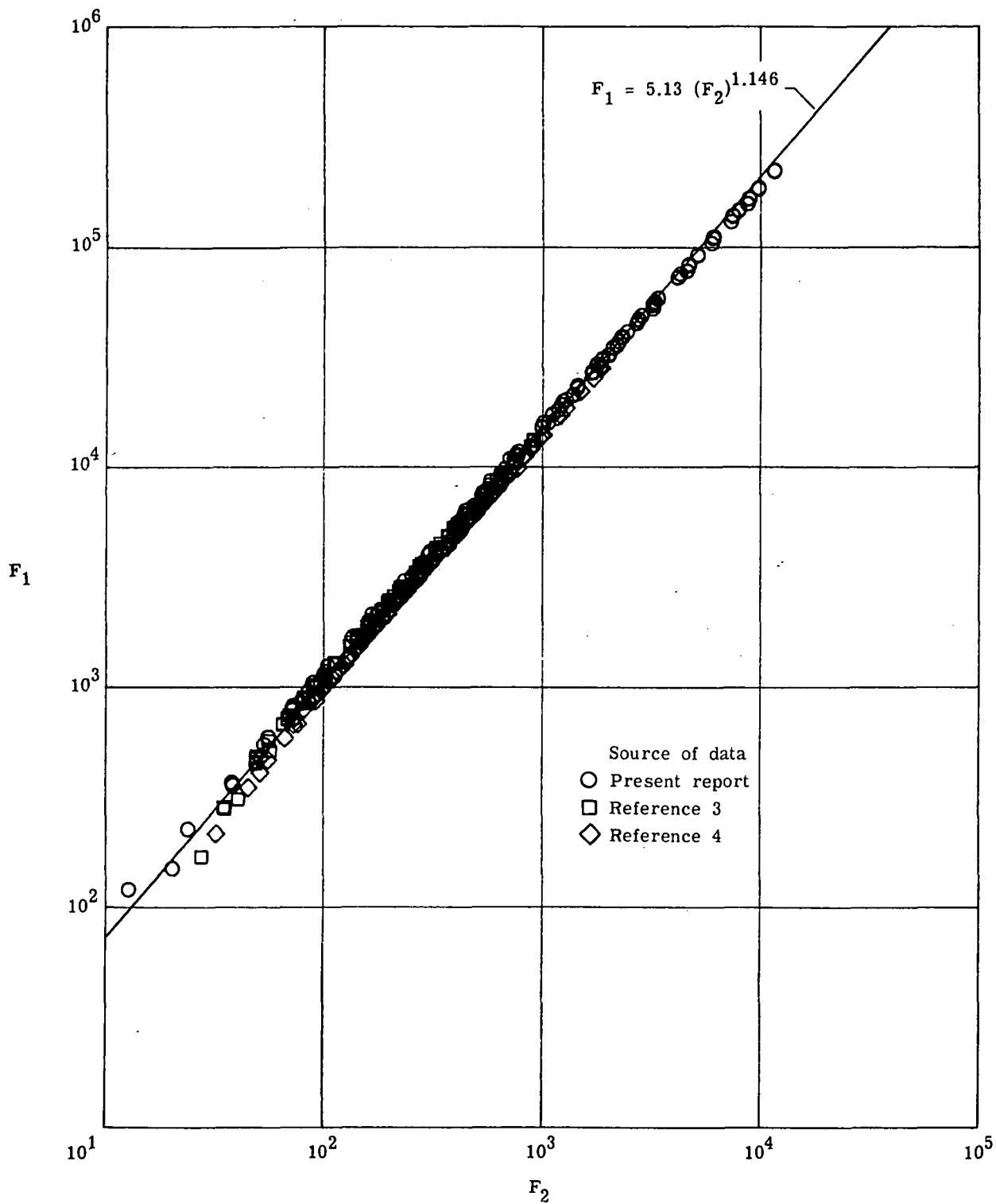
(a) Data collapse.

Figure 2.- Experimental data compared with theoretical values obtained with Fenter-Stalmach equation.



(b)  $c_f$  error.

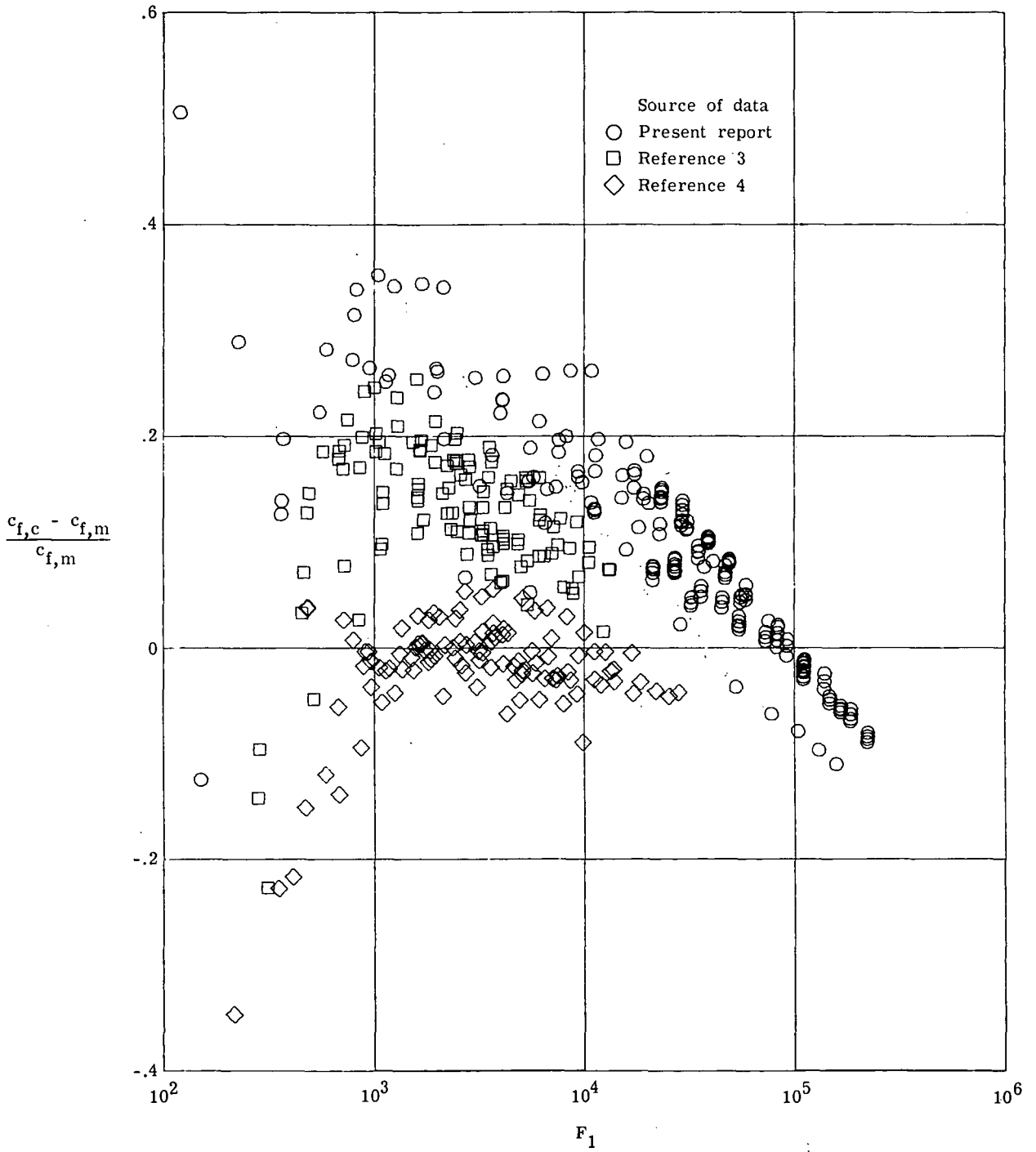
Figure 2.- Concluded.



(a) Data collapse.

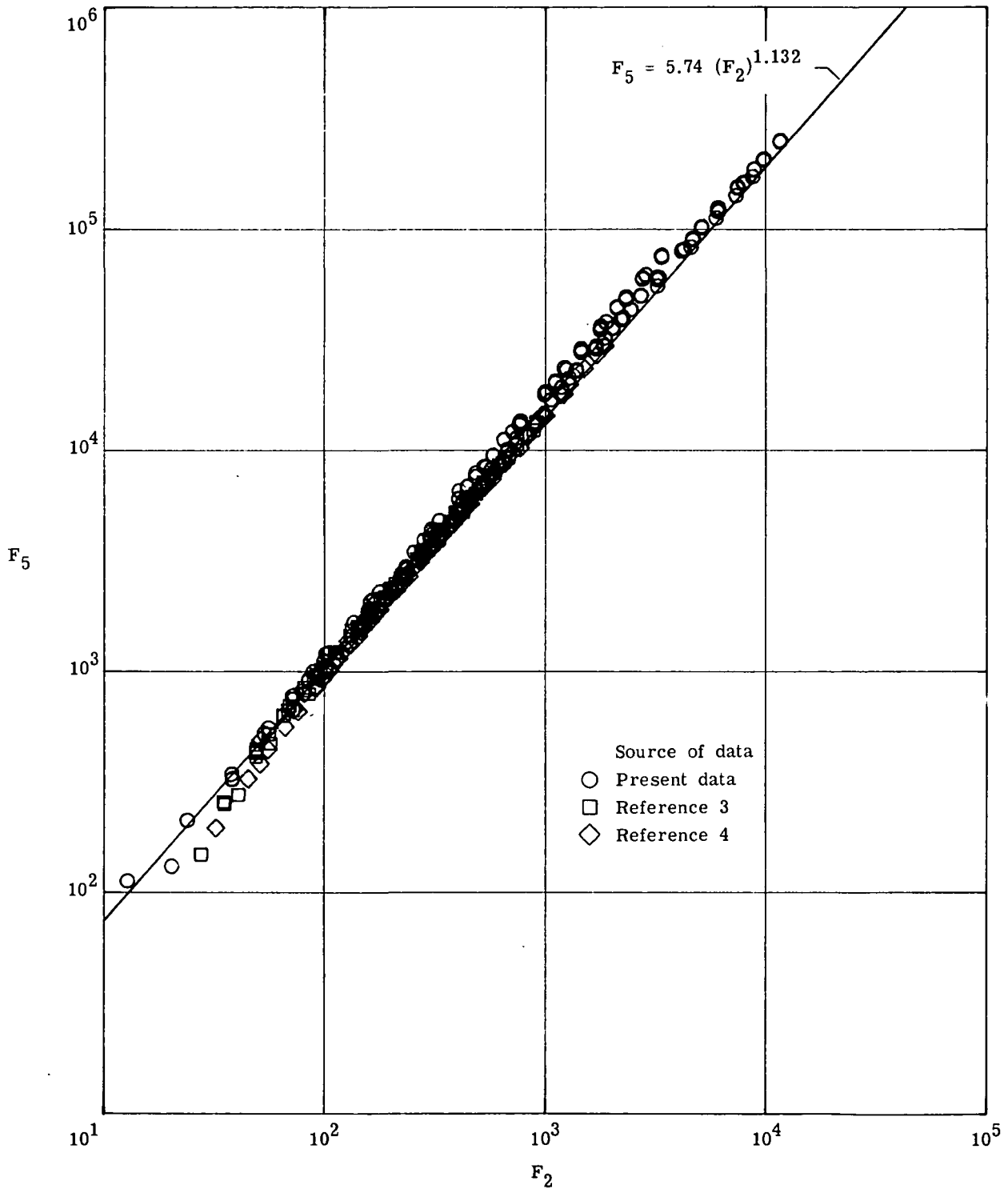
Figure 3.- Experimental data compared with theoretical values obtained with Sigalla equation.





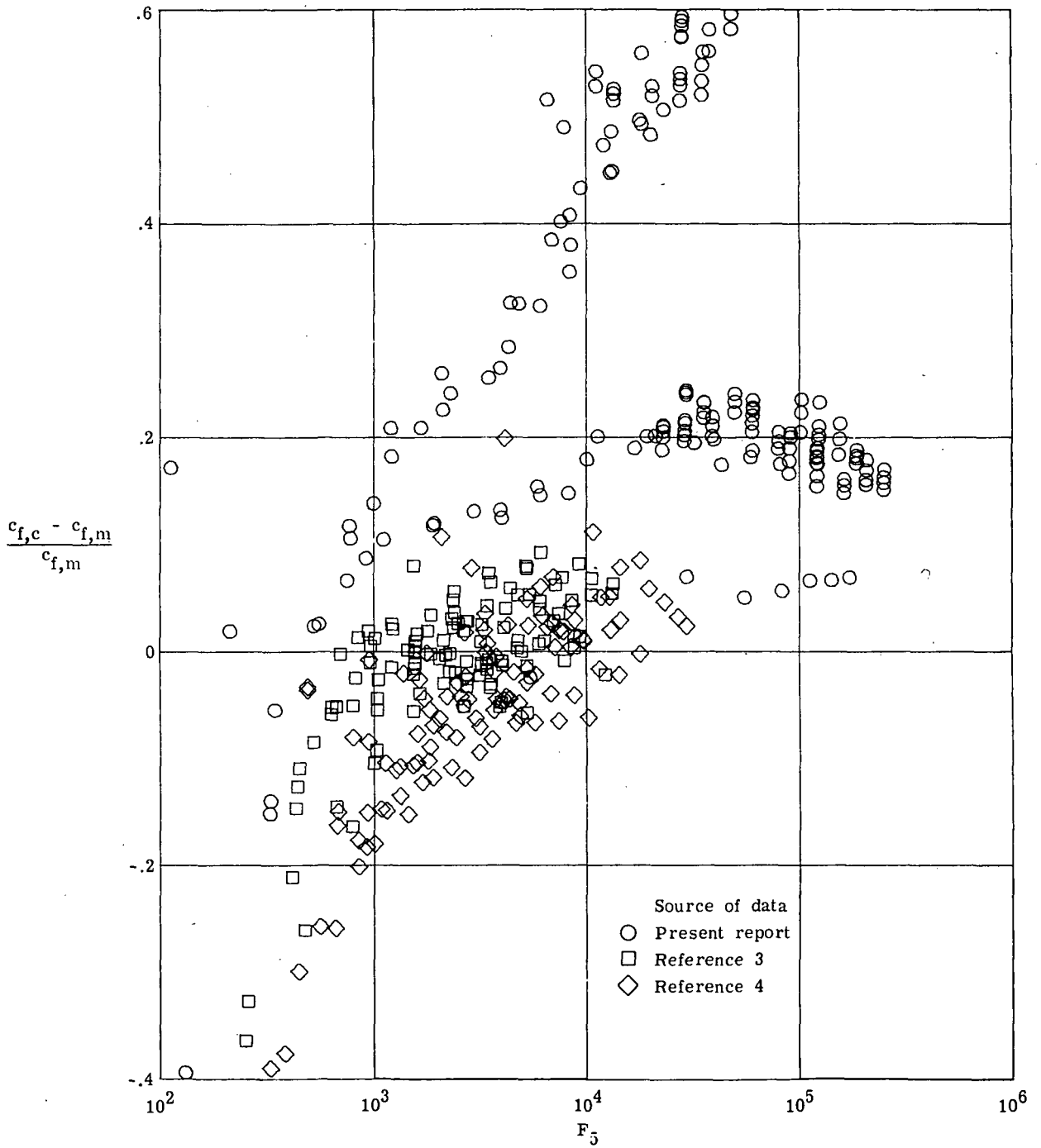
(b)  $c_f$  error:

Figure 3.- Concluded.



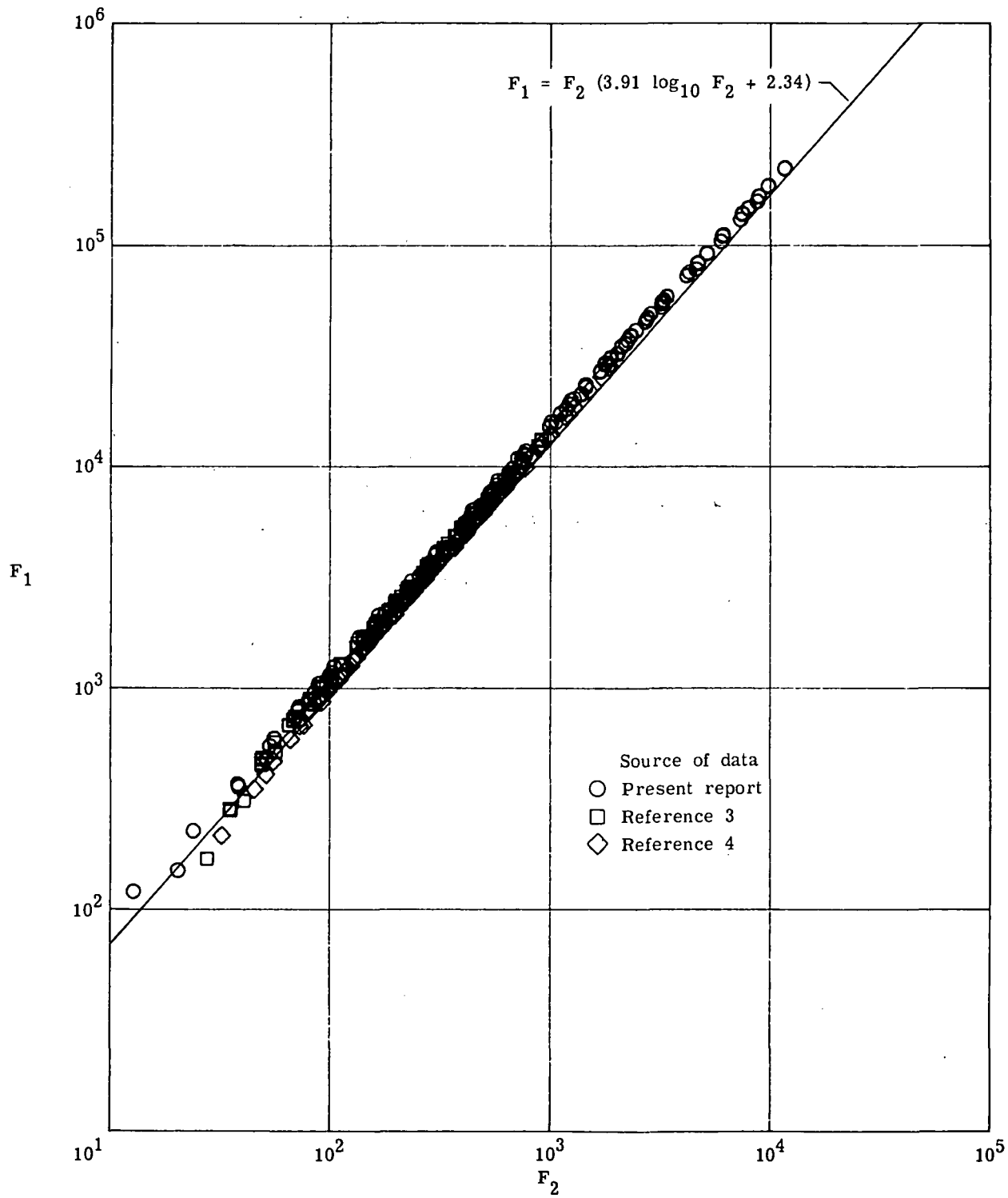
(a) Data collapse.

Figure 4.- Experimental data compared with theoretical values obtained with Hopkins-Keener equation.



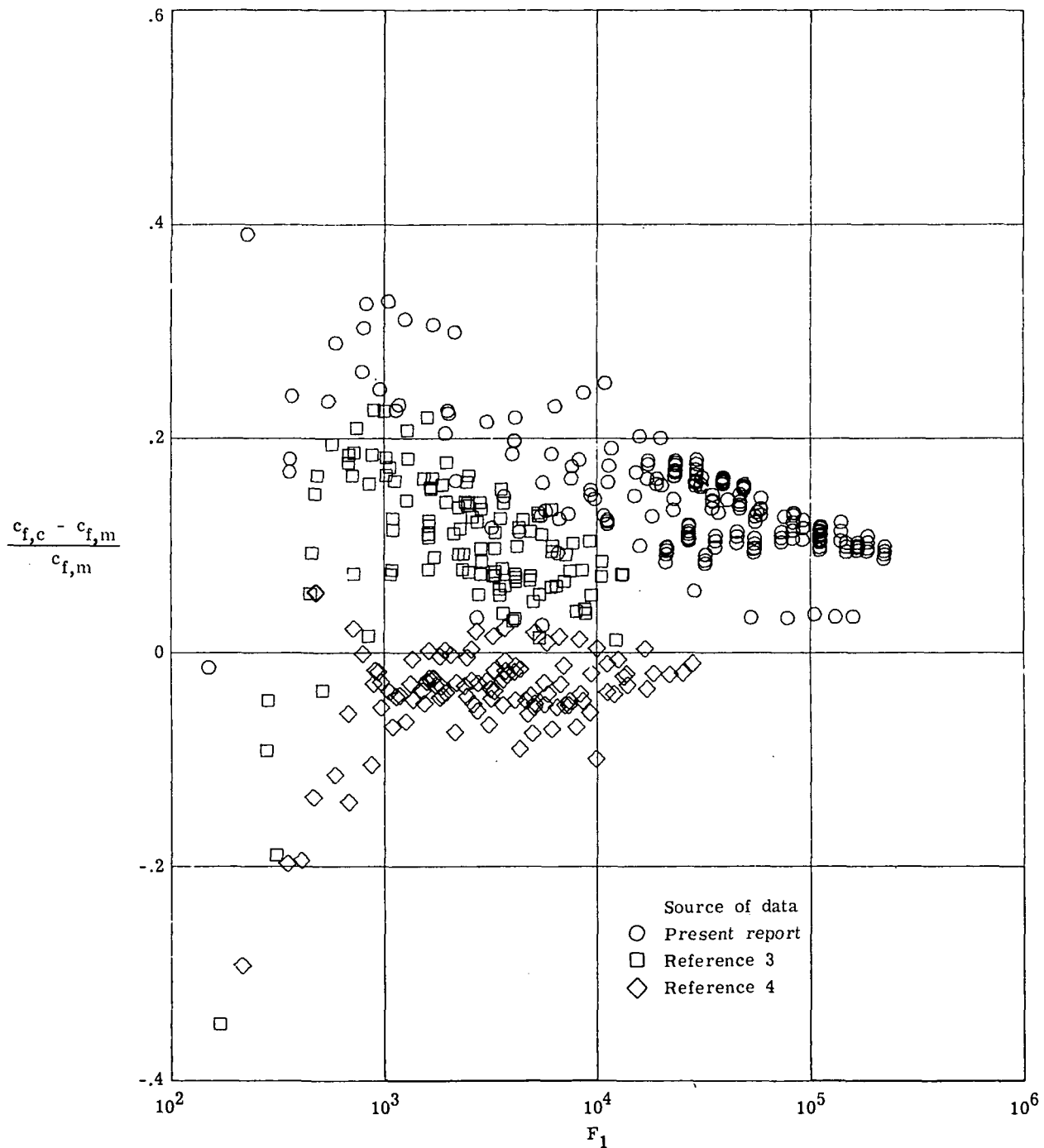
(b)  $c_f$  error.

Figure 4.- Concluded.



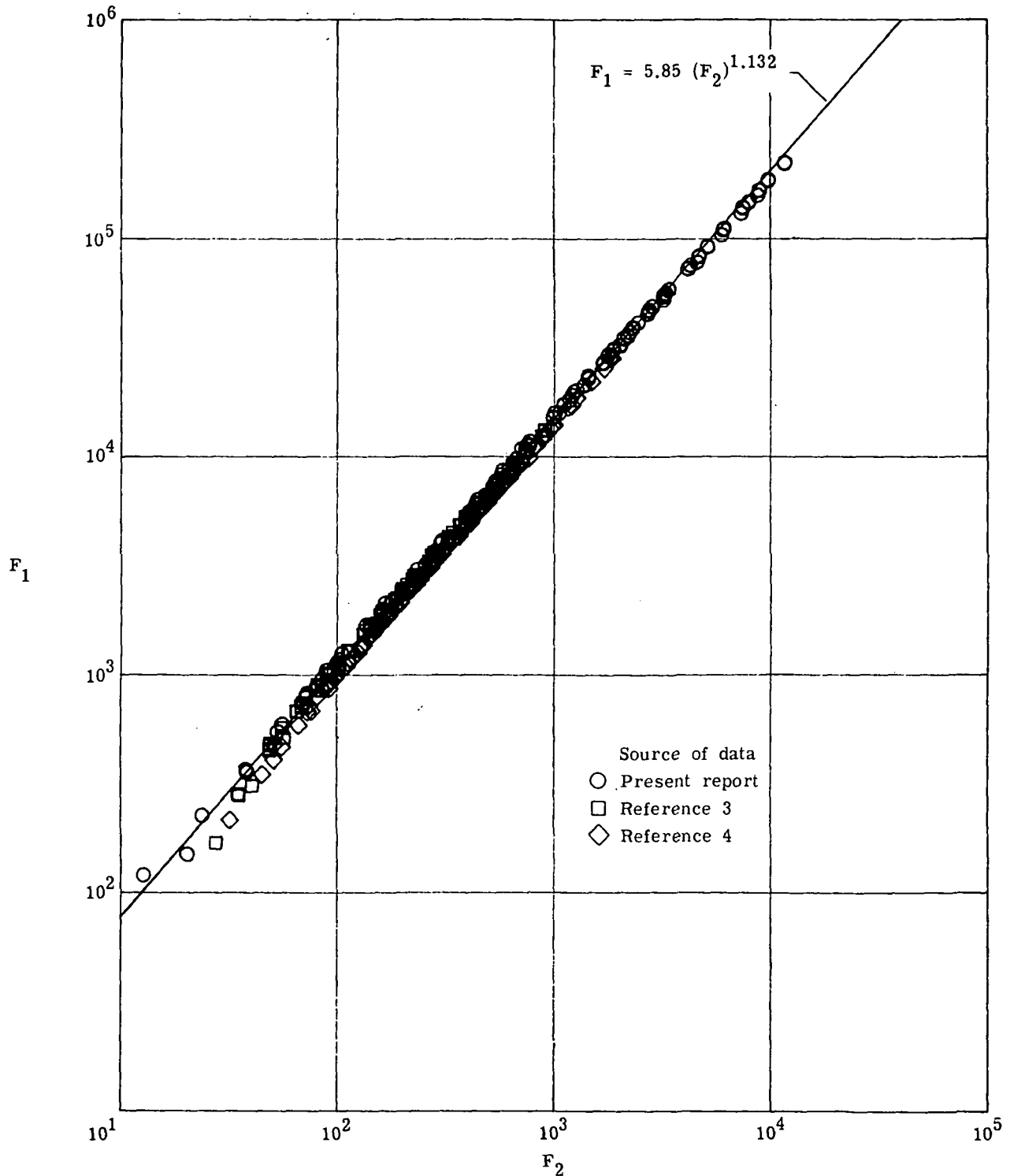
(a) Data collapse.

Figure 5.- Experimental data compared with theoretical values obtained with Patel T' equation.



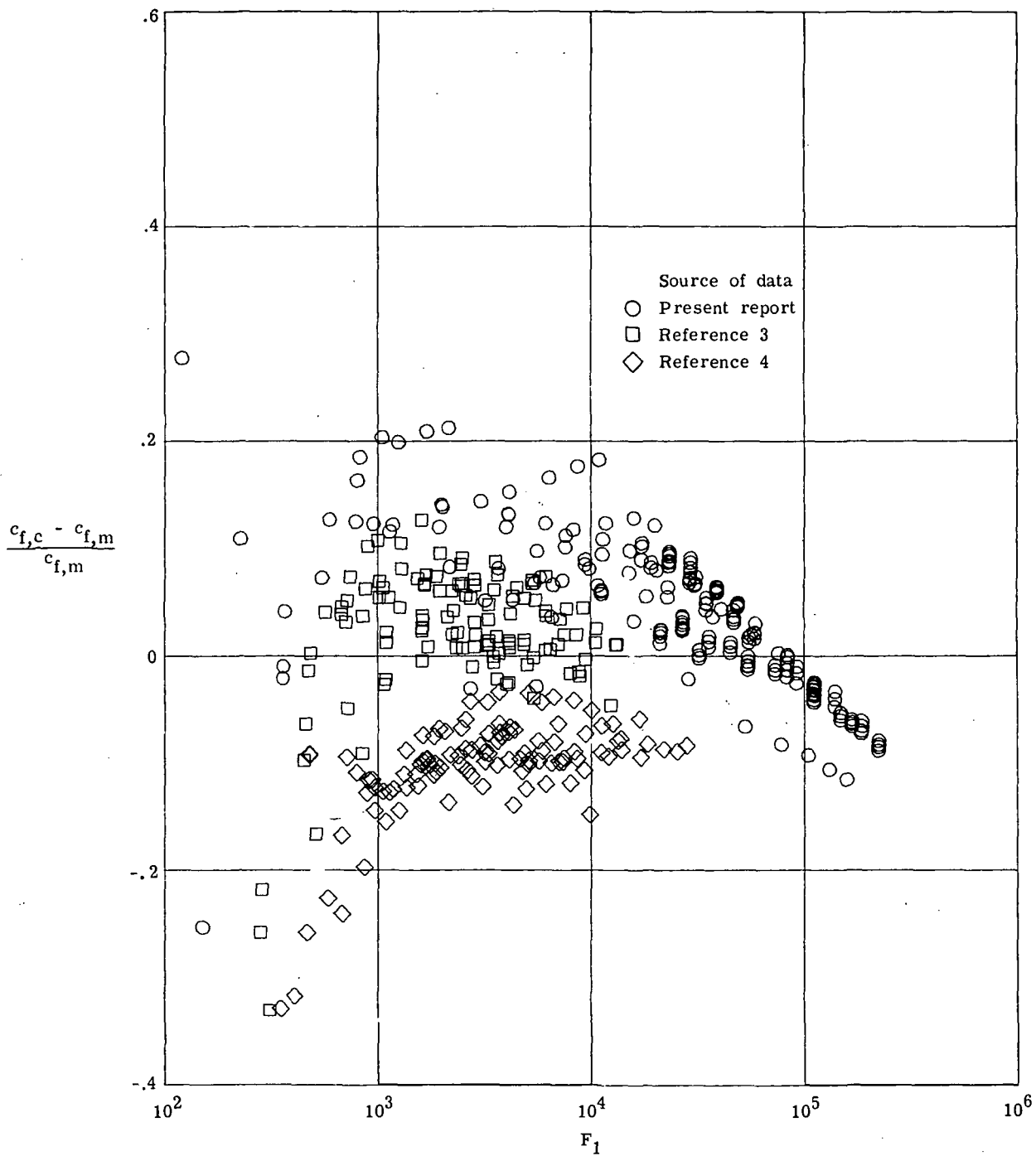
(b)  $c_f$  error.

Figure 5.- Concluded.



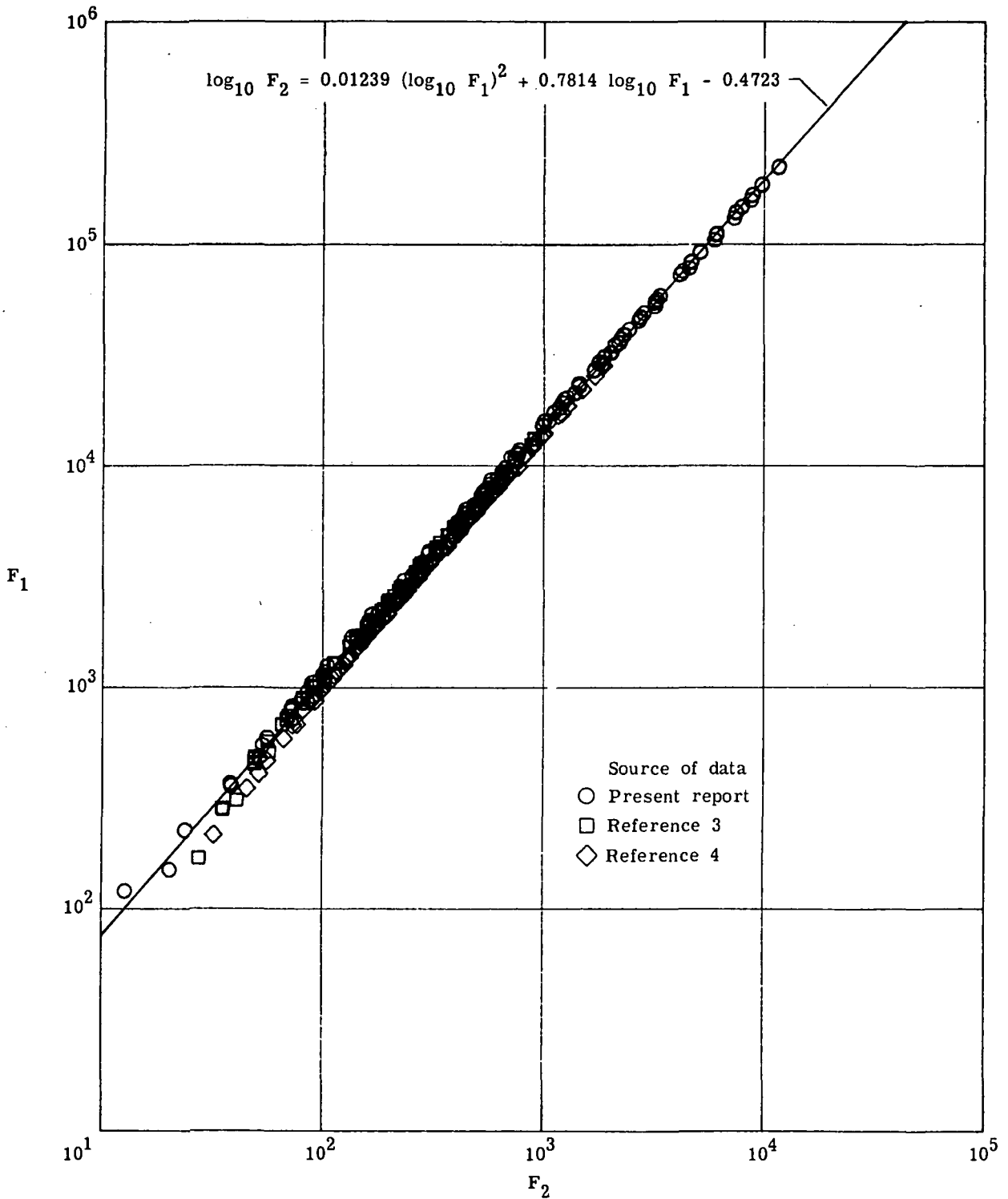
(a) Data collapse.

Figure 6.- Experimental data compared with theoretical values obtained with linear least-squares equation.



(b)  $c_f$  error.

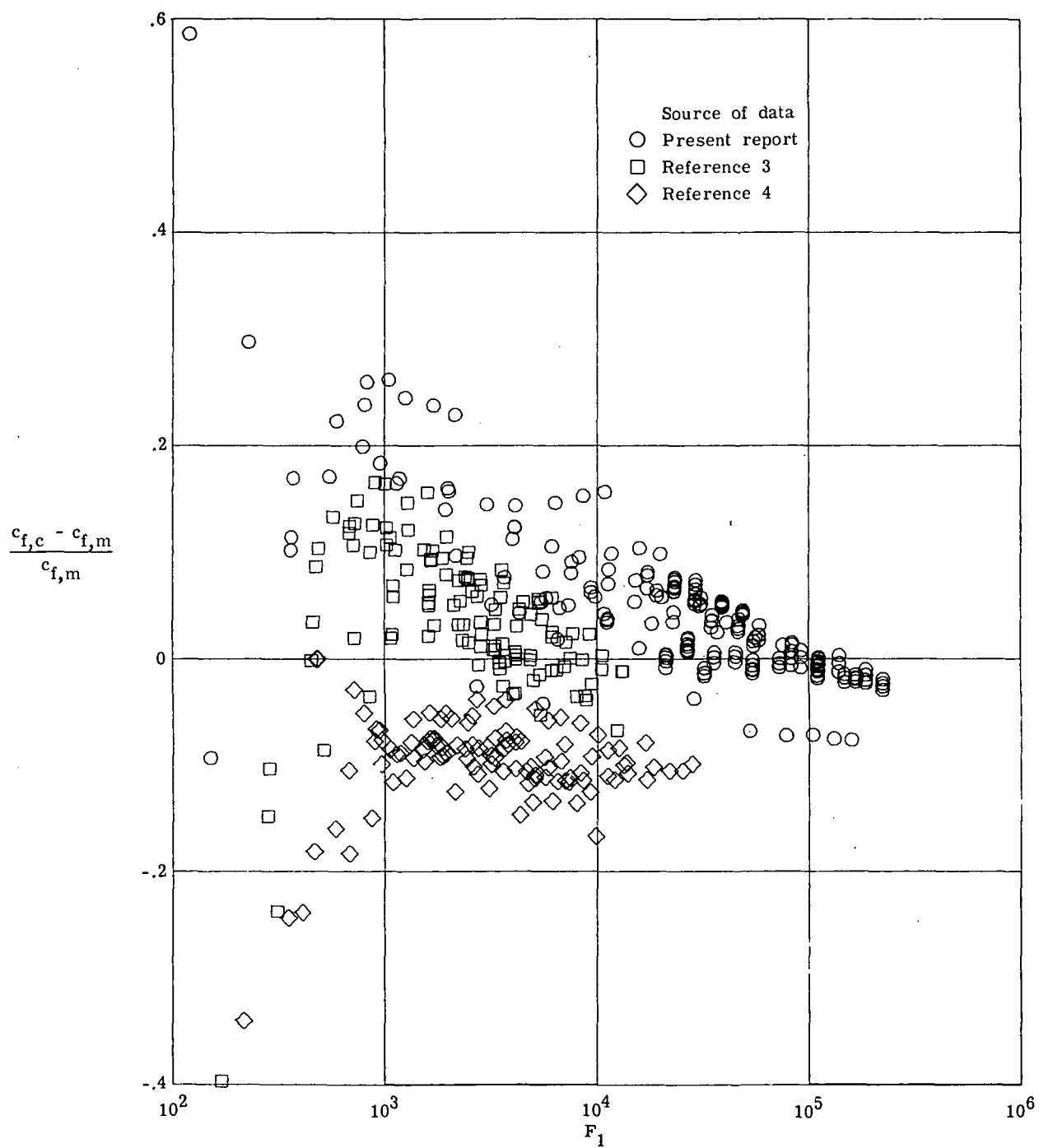
Figure 6.- Concluded.



(a) Data collapse.

Figure 7.- Experimental data compared with theoretical values obtained with second-order least-squares equation.





(b)  $c_f$  error.

Figure 7.- Concluded.

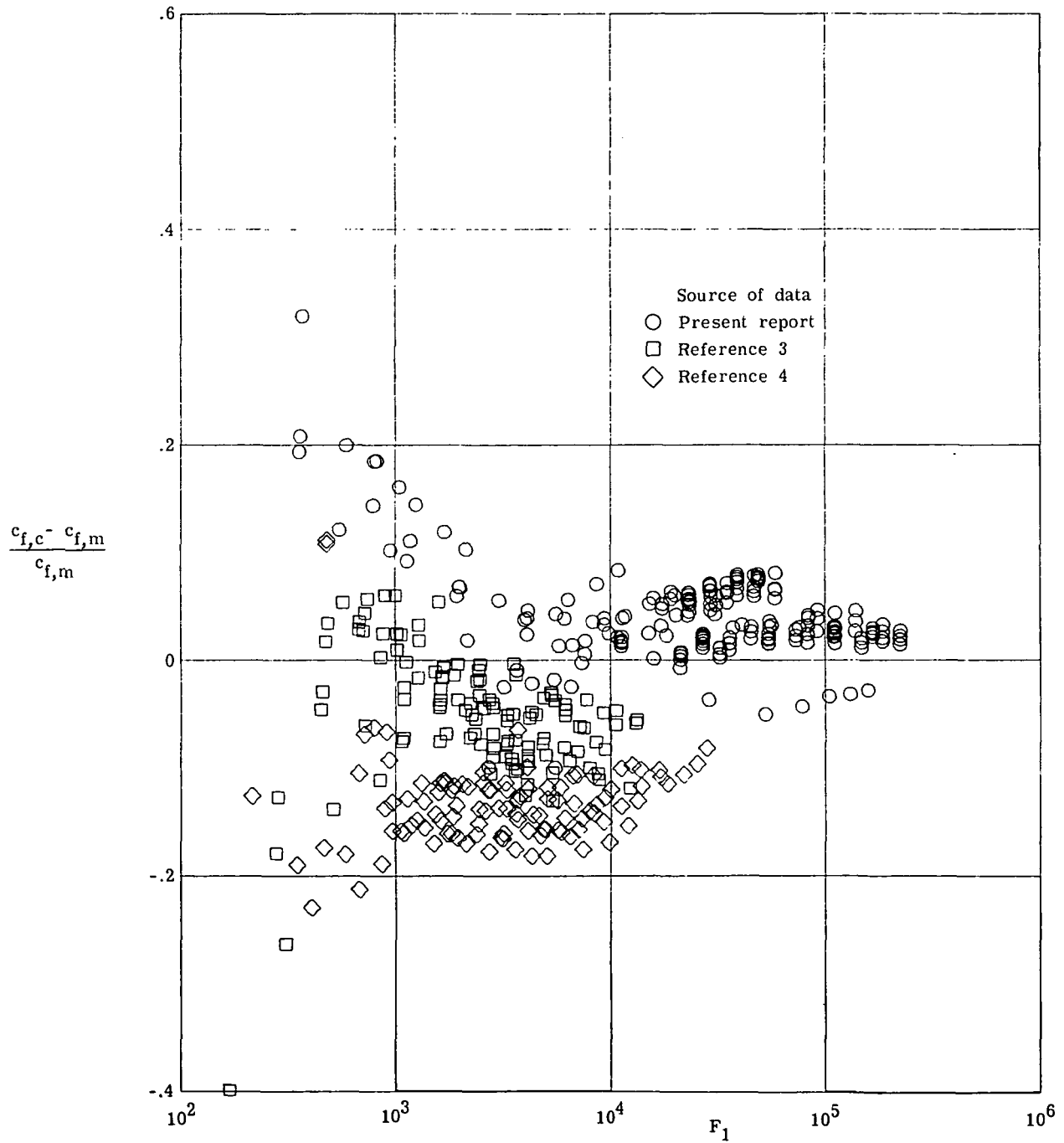


Figure 8.-  $c_f$  error of modified Bradshaw-Unsworth equation.